Adaptive Deconvolution Using a SAW Storage Correlator

JOHN E. BOWERS, STUDENT MEMBER, IEEE, GORDON S. KINO, FELLOW, IEEE, DAVID BEHAR, AND HERMUND OLAISEN

Abstract—**A new analog adaptive filter for deconvolving distorted signals is described in this paper. The filter uses a storage correlator which implements a clipped version of the least mean squared (LMS) algorithm and uses a special iterative technique to achieve fast convergence. The new filter has a potential bandwidth of 100 MHz and would eventually handle pulsed signals of 10-μs width. For signals with time–bandwidth products of less than 100, the adaptation time is less than 1 ms, which allows operation in real time for most applications, including resolution of radar signals in a cluttered environment, removal of echoes from television signals, deconvolution of distorted signals in nondestructive evaluation, and also in telephony. The filter is particularly suited for radar and communications, as it processes signals directly in the VHF range.**

Two experiments related to ghost suppression of a pulse and to the field of NDE are described in this paper. The results are in good agreement with computer simulations and show a ghost suppression of 15 dB for the first example and a sidelobe suppression of 8 dB for a transducer signal. The adaptation time is less than 450 μs.

I. INTRODUCTION

ADAPTIVE FILTERING [1] is useful in removing distortion from signals, particularly when the distortion varies in time. Adaptive filters have been used to perform deconvolution of a distorted echo pulse in an acoustic imaging system [2], to equalize the distortion in a telephone channel [3], and to suppress an interfering signal [4].

Most adaptive filters have been implemented using digital techniques. The limitations of the digital approach are the limited bandwidth (typically 10 MHz) and the practical limit on the number of taps dictated by the complexity and power consumption of systems with large numbers of taps.

An analog–digital hybrid approach has been implemented using MOS LSI technology [6]. This has the advantage of lowering the power consumption and allowing 32 taps to be used without undue external complexity. Large dynamic range was obtained with this technique (60 dB), but the bandwidth was limited to less than 1 MHz.

Most analog implementations of an adaptive filter have been made using CCD's with analog tap weights held in sample-and-hold circuits [7]. The limitations here are the narrow bandwidth and variation across the chip in the gain and threshold levels. The alternative approach used at Hughes for implementing a wide-band adaptive filter is to employ tapped SAW filters with complex computer-controlled systems for adjusting the tap weights [8].

We shall describe here a relatively simple all-analog approach to adaptive filtering which uses the least mean squared (LMS) algorithm to find the optimal set of tap weights. A SAW monolithic ZnO/Si storage correlator with an 8-MHz bandwidth and the equivalent of 24 taps was used [9]. The advantages of this approach are:

1) fast iteration rate (100 kHz), which means a short learning time ($\sim$100 μs) and good ability to track time varying signals;
2) simple external connections;
3) large potential bandwidth (100 MHz);
4) large potential number of taps (1000);
5) lower power consumption (0.1 W);
6) it is suited for radar and communications systems because it can operate directly at the IF frequency.

A disadvantage is that, at the present time, the dynamic range is less than for digital systems.

A brief introduction to the LMS algorithm is provided, followed by a new derivation of the LMS algorithm. As the class of applications discussed here utilizes continuous, quasi-static filters, a derivation in the frequency domain rather than the time domain allows more physical insight into the processing capability of the LMS algorithm and into its advantages and limitations for these kinds of applications.

Two adaptive deconvolution experiments which used the storage correlator are described. In the first experiment, an undesirable time-delayed ghost pulse is removed. In the second experiment, the ringing in the pulse response of an acoustic transducer is removed by adaptive filtering. The results of these experiments are compared to computer simulations with the LMS algorithm. Conclusions are drawn regarding which properties and nonlinearities of the storage correlator limit the performance of the adaptive filter.

Manuscript received February 4, 1980; revised July 7, 1980. This work was supported by the Defense Advance Research Projects Agency and monitored by the Office of Naval Research under Contract N00014-76-C-0129.

J. E. Bowers and G. S. Kino are with Ginzton Laboratory, Stanford University, Stanford, CA 94305.

D. Behar was with Ginzton Laboratory, Stanford University, Stanford, CA. He is now with the Israeli Ministry of Defense, P.O.B. 2250, Haifa, Isreal.

H. Olaisen was with Ginzton Laboratory, Stanford University, Stanford, CA. He is now with the Norwegian Defense Research Establishment Division for Electronics, 2007 Kjeller, Norway.

0018-9480/81/0500-0491$00.75 ©1981 IEEE

II. Experimental Procedure

A. The LMS Algorithm

Consider an adaptive filter with an input $x(t)$ and output $y(t)=x*w$, where $*$ indicates convolution. The weight function is adjusted after each iteration such that the output $y(t)$ converges to a desired signal $d(t)$. The time it takes for convergence to occur is commonly called the learning or training time. After the optimum set of weights w is determined, the filter can be used to remove the distortions in signals. For example, in a TV system with a ghost, the filter can be trained on the sync signal (which occurs at the beginning of each line) to remove the echo sync signal, and then the entire TV line can be passed through the filter, and the "ghosts" will be removed.

The error $\epsilon(t)$ between the desired signal $d(t)$ and the output of the filter $y(t)$ is

$$\epsilon(t)=d(t)-y(t) \tag{1}$$

where

$$y=x*w. \tag{2}$$

The LMS algorithm specifies that to minimize error, w must be changed by Δw such that

$$\Delta w=2\mu x\bigstar\epsilon \tag{3}$$

where $\bigstar$ indicates correlation and 2μ is a constant which determines the rate of convergence of the system. Thus it follows from (1)–(3) that

$$\Delta w=2\mu x\bigstar(d-x*w). \tag{4}$$

A proof is given in the following section that if these adjustments in Δw are made, then the weighting function exponentially approaches the Wiener filter solution; this is a filter which minimizes the average mean square error (mse), over the frequency band of interest, between the output signal and the desired signal d.

It can be seen from the expression for the weighting function adjustment [(4)] that for each iteration, a convolution with x, and a correlation with x must be performed. In addition, an analog storage register is needed for w, and it must be possible to adjust the weighting function.

The SAW storage correlator is ideally suited for this purpose, as it can perform all of these operations (convolution, correlation, addition, and storage). All of the necessary operations are performed inside a two- (or three-) port device in real time. A big advantage of this approach is its simplicity.

B. The Storage Correlator

The SAW storage correlator is a device which utilizes the interaction between a propagating surface acoustic wave and a charge distribution stored in an array of diodes to store, correlate, or convolve two broad-bandwidth signals in real time. A series of signals may be added together by successively storing them in the diode array. A brief description of the storage correlator follows. Complete descriptions of the device [10], [11] and its operation [12], as well as a theory of the device [13], are given in the literature.

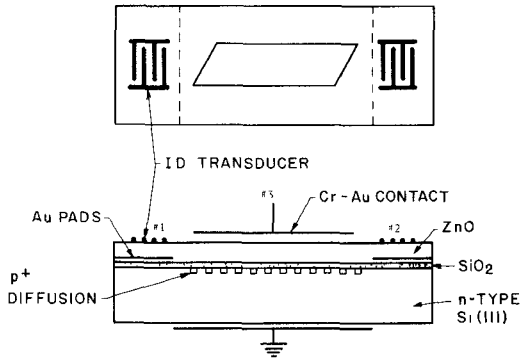

Fig. 1. Schematic drawing of storage correlator.

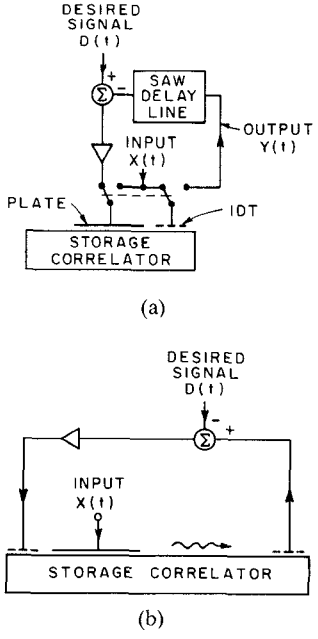

Fig. 2. (a) Actual and (b) proposed implementation of SAW adaptive filter.

A schematic drawing of a storage correlator is shown in Fig. 1. If a modulated carrier x is applied to the acoustic port (2), and a signal ϵ to port 3, then the charge distribution [13]

$$\Delta w=2\mu x\bigstar\epsilon \tag{5}$$

is added to the charge distribution w, stored in the diode array. If a signal x is then applied to port 3, then the convolution

$$y=x*w \tag{6}$$

is the output at port 2. The LMS algorithm can be realized by repeating the process many times. Eventually, the weighting function w converges to an approximation to the Wiener solution, and the programming is complete. The filter may then be used to deconvolve other signals which have been distorted in the same manner.

The external connections used to operate the storage correlator are indicated in Fig. 2(a). A much simpler method

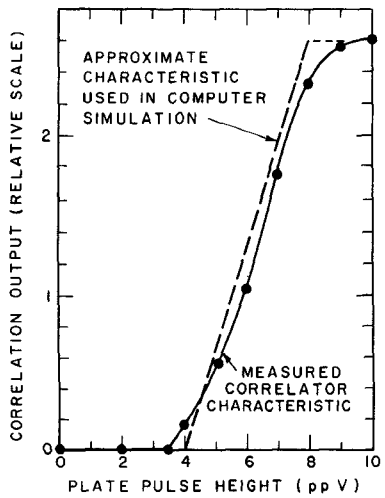

Fig. 3. Correlator output as a function of plate (readout) pulse height.

is indicated in Fig. 2(b) where two acoustic ports of the correlator are used, and the external delay line and switches are not needed. A difference amplifier is not needed to subtract $d(t)$ and $y(t)$; rather the carrier frequency is adjusted so that there is a phase difference of π between the delayed signal $y(t)$ and the desired signal $d(t)$. This is explained more fully in the next section.

The storage correlator is not an exact implementation of the Widrow-type LMS adaptive filter since the effect of the plate signal (port 3) on the weighting function is not linear (Fig. 3). If the error signal is less than a threshold determined by the characteristics of the device (4 V), the weighting function is unaffected. The error signal is clipped around 9 V, so only $\sim$6 dB of the dynamic range is available at port 3. If the error signal is fed into an acoustic port (as in Fig. 2(b)), then at least a 35-dB dynamic range should be available.

The weighting function $w(z)$ is stored in 2000 diodes, however, the equivalent number of taps is much less since the charge stored on each diode cannot be independently modified. The bandwidth is 8 MHz and the maximum signal duration is 3 μs; consequently, the time–bandwidth product or equivalent number of taps is 24. For the computer simulations, the device was represented in the computer by a 24-tap transversal filter. The necessary correlations and convolutions were calculated in the computer, and the error signal was modified according to the transfer characteristic shown in Fig. 3. It can be seen that this transfer characteristic closely approximates the experimentally observed characteristic.

III. Theory

A. Introduction

The LMS algorithm has been analyzed in detail by Widrow [14], [15]. The first task in his analysis is to transform from the coordinate system consisting of N samples from the waveform to a set of normal coordinates where the correlation matrix is diagonal, the eigenvectors of the correlation matrix are mutually orthogonal, and, most importantly, the decay modes are uncoupled. Once this transformation is accomplished, expressions for the decay constants τ_p, misadjustment, etc., may be derived.

In the analysis presented here, the transformation is very easily accomplished by taking the Fourier transform of all quantities. Correlations are then simple products, and the convergence of a quantity at a given frequency is independent of other frequencies, i.e., the modes are uncoupled.

B. Convergence

Consider the situation in Fig. 2 where all signals are RF modulated, and the carrier frequency is ω_0. The desired signal $d_n(t)$ and the input signal $x_n(t)$ are repetitive, and as the number of iterations n increases, the only change in these signals is a phase change

$$d_n(t)=d(t)e^{j\omega_0 nT} \tag{7}$$

where T is the iteration time. In the frequency domain

$$D_n(\omega)=D(\omega)e^{j\omega_0 nT}. \tag{8}$$

Similar expressions hold for the distorted signal $X(\omega)$.

The filter output is

$$Y_n(\omega)=X(\omega)W_n(\omega)e^{j\omega_0(nT+T_0)} \tag{9}$$

and the error signal is

$$\begin{aligned} E_n(\omega)&=D_n(\omega)+Y_n(\omega)e^{-j\omega_0 T_D}\\ &=D(\omega)e^{j\omega_0 nT}+X(\omega)W_n(\omega)e^{j\omega_0(nT+T_0-T_D)} \end{aligned} \tag{10}$$

where T_D is the length of the external delay line, and T_0 is the delay time before $x(t)$ is applied to the plate port. In Fig. 2, T_0 is zero.

The weight adjustment is

$$\Delta w(t)=2\mu_a X(t)\bigstar\epsilon_n(t). \tag{11}$$

Equivalently, we can write

$$\begin{aligned} W_{n+1}(\omega)&=W_n(\omega)+2\mu E_n(\omega)_a X_n^*(\omega)\\ W_{n+1}(\omega)&=AW_n(w)+B \end{aligned} \tag{12}$$

where a superscript $*$ indicates a complex conjugate and

$$\begin{aligned} A&=1+2\mu X(\omega)X^*(\omega)e^{j\omega_0(T_0-T_D)}\\ B&=2\mu D(\omega)X^*(\omega). \end{aligned} \tag{13}$$

Equation (12) has the solution

$$W_n(\omega)=(W_i-W_w)A^n+W_w \tag{14}$$

where W_i is the initial weight distribution and

$$W_w=\frac{D(\omega)}{X(\omega)}e^{j\omega_0(T_0-T_D)}. \tag{15}$$

Equation (14) converges only if $|A|<1$. The fastest convergence is obtained for the carrier frequencies where the error signal is the subtraction of D and Y, i.e., when

$$\omega_0=\frac{\pi}{|T_D-T_0|}(2p+1) \tag{16}$$

where p is an integer. If the feedback gain μ is sufficiently small

$$\mu < \frac{1}{XX^*} \tag{17}$$

then the convergence requirement $|A|<1$ is satisfied for carrier frequencies in bands of width $\Delta\omega$ around the frequencies given by (16), where

$$\Delta\omega = \frac{2}{|T_D - T_0|} \arccos(\mu XX^*). \tag{18}$$

It can be seen from (17) that when μ is near its upper limit, the carrier frequency must be close to one of the values given by (16).

If the feedback gain is significantly less than its maximum value, it follows that

$$A = 1 + 2\mu XX^* e^{j\omega_0(T_0 - T_D)} \approx e^{-1/\tau} \tag{19}$$

where

$$1/\tau = 2\mu XX^* e^{j[\omega_0(T_0 - T_D)+\pi]}. \tag{20}$$

The convergence of the weighting function [(14)] is approximately exponential. Thus we can write

$$W_n \approx (W_i - W_w)e^{-n/\tau} + W_w. \tag{21}$$

The error is

$$E_n = D - XW_n$$

$$E_n \approx X^*(W_i - W_w)e^{-n/\tau}. \tag{22}$$

The error decays exponentially to zero. In practice, the bandwidth of the system is limited by the bandwidth B of the acoustic transducers. Consequently, the error outside this frequency range is not affected by the adaptation process. It will also be noted that phase distortion in the system is cancelled out by the application of the convolution and correlation process in turn. Thus although this is basically a feedback system, there is no problem with instability, provided the convergence criteria are satisfied.

We have implicitly assumed that the signals $x(t)$ and $d(t)$ are sufficiently short compared to the time length of the diode array that all of the nonzero portion of the signal is stored in the diode array. Then, the error at every frequency decays independently of every other frequency. Furthermore, the error decays to zero (22). However, suppose part of $\Delta w(z)$ is not stored

$$\Delta w(z) = \begin{cases} 2\mu x \bigstar \epsilon_n, & \text{where } |t| < T_s/2 \\ 0, & \text{otherwise} \end{cases} \tag{23}$$

where T_s is the maximum stored signal duration. Then, the different frequencies do not decay independently, and the analysis is more difficult. An important result of this more difficult case is that the error does not decay to zero.

If noise on the input signal X is included in the analysis, and if the noise on the plate and acoustic ports is correlated, as they would be if a delay line were used to generate the second X signal which is needed during each iteration, the expression for the convergence of the weighting function is again given by (22) where

$$W_w = \frac{DX^*}{XX^* + \langle NN^* \rangle} \tag{24}$$

and

$$\tau = \frac{1}{2\mu(XX^* + \langle NN^* \rangle)}. \tag{25}$$

Equation (24) is, of course, the Wiener filter solution.

IV. Results and Discussion

A. Echo Suppression

In this experiment, a square pulse 0.4 μs long is followed by an echo pulse. The desired signal is a single pulse 0.4 μs long. For an echo which is 6 dB less in amplitude than the main pulse (Fig. 4(a)), the sidelobe suppression after 10 iterations (200 μs) is 15 dB, as shown in Fig. 4(b). The dependence of sidelobe suppression on echo height is shown in Fig. 5. The results of computer simulations of the LMS algorithm with 24 taps and using clipping and threshold 6 dB below the clipping level are also shown in Fig. 5. The computer simulation agrees very well with experimental results, except that the maximum sidelobe suppression is 23.5 dB, which is 4.5 dB higher than was experimentally obtained. The reason is that the spurious signals generated in the device during readout limit the dynamic range of the signal output.

An important result obtained in this experiment is that spurious acoustic signals generated by the plate readout signal can be suppressed by up to 13 dB as a result of the adapting process. The filter does not distinguish between echoes and distortions generated externally or by the device itself. This result is demonstrated in Fig. 6. The upper trace is the adaptive filter result after removing an echo from a 0.4-μs-long pulse. If all signals except the plate readout signal are removed, the filter output (lower trace) is the spurious signal generated by the plate signal. A large spurious signal can be seen when previously there had been a null.

The advantage of computer simulation of this adaptive filter is that the threshold and clipping levels may be easily changed to see what effect they have on the preformance of the adaptive filter. These results are summarized in Table I. The computer simulated linear LMS result is given in the first row. If a threshold level is included, then the computer simulation converges much faster, but to worse results. The values obtained are in agreement with experimental results. If the feedback gain is increased so that the error signal is now clipped, then much better sidelobe suppression is obtained in both the experimental and computer simulation cases. We note that clipping of the signal increases the rate of convergence radically, as has been noted by others. The algorithm employed is, therefore, known as the clipped LMS algorithm.

Regardless of the shape of the desired signal (d) and the input signal (x), it was *always* experimentally observed that the feedback gain must be large enough to strongly

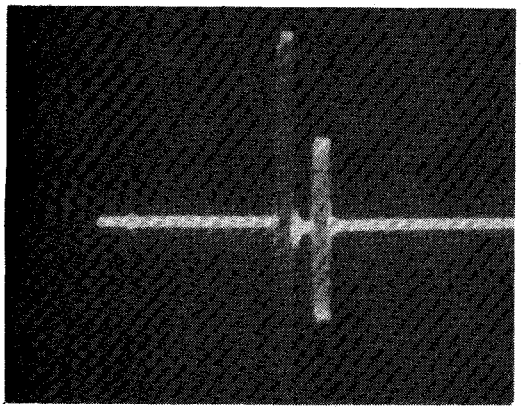

(a)

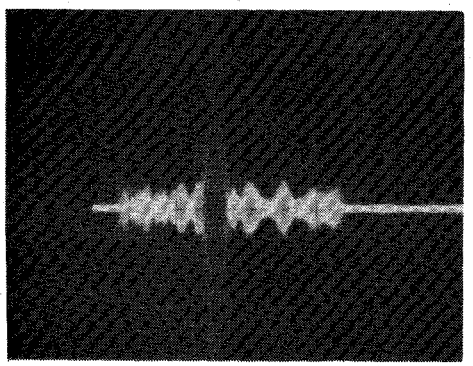

(b)

Fig. 4. (a) Input signal and (b) output signal after 22 iterations. 1 division = 1 μs.

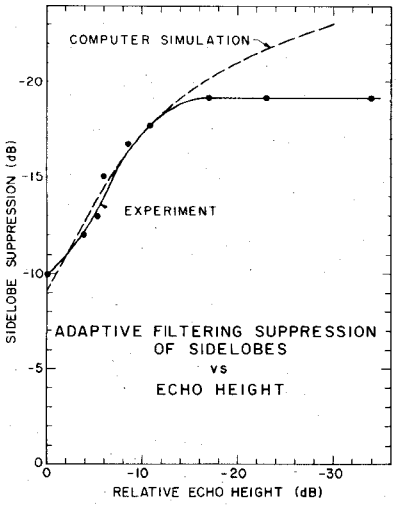

Fig. 5. Experimental and computer simulation results for echo-suppression experiment.

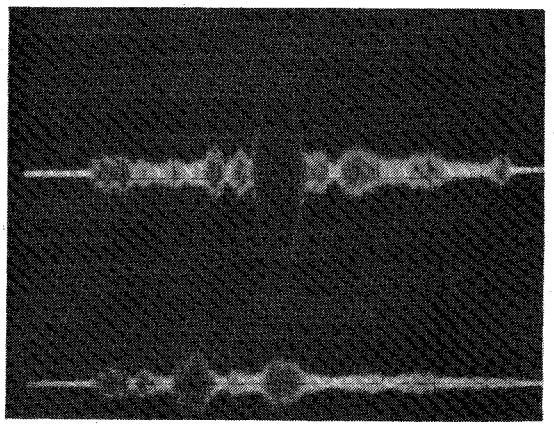

Fig. 6. Echo reduction after 10 iterations (upper trace). Spurious signals generated by plate readout signal (lower trace).

TABLE I
EXPERIMENTAL RESULTS AND COMPUTER SIMULATIONS FOR A FILTER INPUT OF A 0.4-μs WIDE PULSE WITH A -6-dB ECHO (THE COMPUTER SIMULATION USES 24 TAPS)

	STORAGE CORRELATOR RESULTS		COMPUTER SIMULATION	
	Sidelobe Suppression (dB)	Number of Iterations for Convergence	Sidelobe Suppression (dB)	Number of Iterations for Convergence
Linear	---	---	14.0	25
Threshold*	10.0	5	10.7	4
Threshold and Clipped	14.8	10	14.2	6

*The maximum feedback signal (e) was not more than 6 dB above the threshold level.

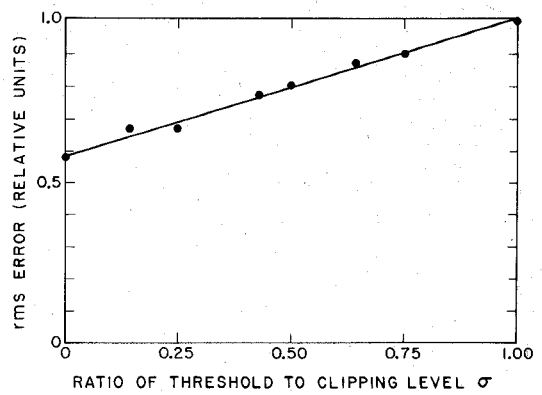

Fig. 7. Minimum rms error as a function of threshold level.

clip the error signal during the first few iterations for the optimum filtering. After many iterations, the error signal is only slightly clipped.

The threshold and clipping levels can be changed by modifying the design of the storage correlator. For this reason, a series of computer simulations was made to determine the effect of having other threshold to clipping ratios (σ) than $\sigma = 0.5$ which exists in the present devices. Only the ratio σ is important here. The minimum rms error does not change if the threshold, clipping, and gain values are all multiplied by the same value. The asymptotic value of the rms error is shown as a function of σ in Fig. 7 for the case of a 6-dB echo. The optimum value of the gain is used at each point. The end point $\sigma = 1.0$ corresponds to the situation of hard clipping where the threshold level equals the clipping level, and the feedback error is either 1 or 0.

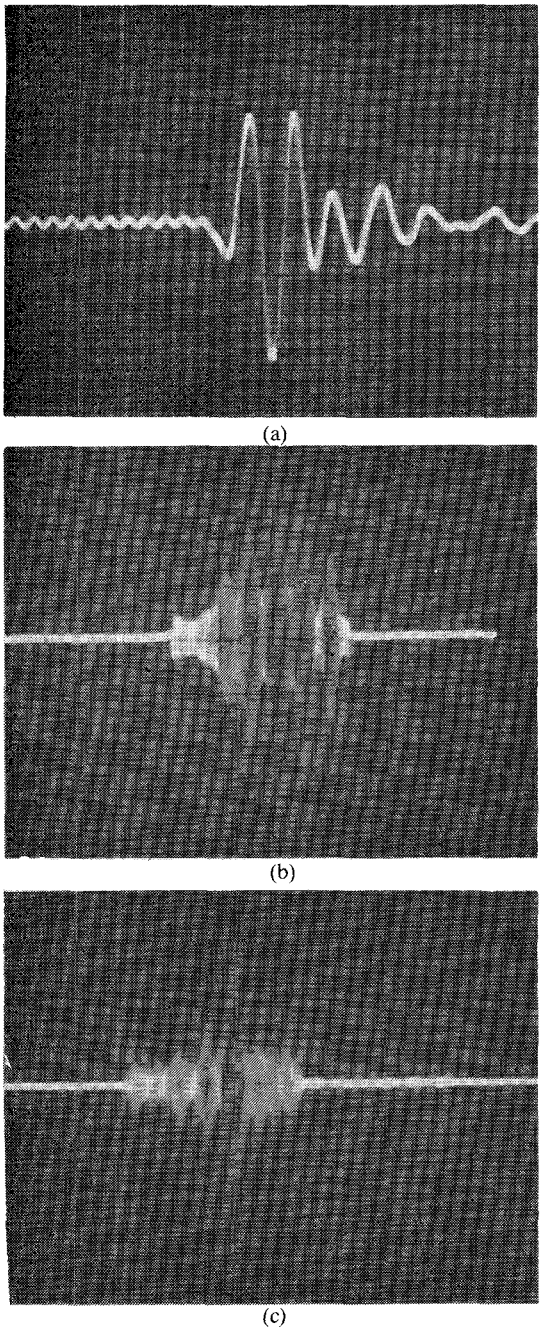

Fig. 8. (a) Impulse response of 1.25-MHz bulk acoustic transducer; (b) autocorrelation of impulse response; and (c) filter output after 10 iterations of adapting. 1 division = 1 μs.

The rms error increases linearly with σ. This is intuitively expected since any error values less than the threshold do not affect the tap weights and are not adapted to zero. The rms error would then linearly increase with threshold level. Consequently, the design of the storage correlator should minimize the threshold value.

B. Reduction of Bulk Transducer Ringing

The object of this experiment was to improve the impulse response of an acoustic bulk wave 1.25-MHz transducer used for acoustic nondestructive evaluation. The impulse response is shown in Fig. 8(a). The desired signal is a unipolar pulse with a width of 0.3 μs. If the impulse response is correlated with itself (Fig. 8(b)), the highest sidelobe is 1.7 dB smaller than the peak. However, if the correlator is used as an adaptive filter, then the sidelobe level can be reduced to 7 dB below the peak after 10 iterations (Fig. 8(c)) and 10 dB below the peak after 35 iterations.

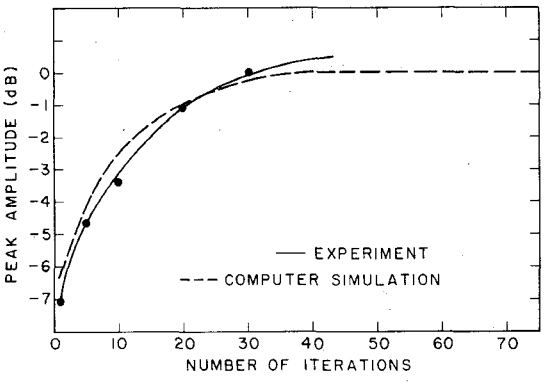

Fig. 9. Output pulse level during adapting process.

The growth of the peak as the number of iterations increases is shown in Fig. 9. The computer simulation is also shown and can be seen to be in good agreement with the experimental result, except that the maximum predicted suppression is 2.6 dB better than was experimentally observed.

Linear LMS theory predicts [1] that the time-averaged error should decay exponentially to a constant value. The ratio of this constant value to the Wiener solution is called the misadjustment M. The misadjustment is approximately related to the decay constant τ by the relation [1]

$$M = N/4\tau \tag{26}$$

where N is the number of tap weights. In our case, N is the time–bandwidth product of the storage correlator. Thus the faster the convergence, the larger the misadjustment.

The experimentally observed decay of the mse for the bulk transducer case is shown in Fig. 10. The decay is exponential, except for the first few iterations when the error signal is strongly clipped and the mse decays faster than an exponential. The experimental decay constant is 7.5, and the misadjustment calculated from (26) is equal to 0.8. We interpret this to mean that the final result is close to the Wiener solution.

C. Limitations

The bandwidth of this device (8 MHz) is larger than the bandwidth of most other methods of implementing the LMS algorithm, however, larger bandwidths are often desirable. For instance, our technique can work well as an adaptive filter for a 1.25-MHz transducer, but it works poorly for a 2.5-MHz transducer. The bandwidth limitation in this device is the result of the low surface-wave coupling coefficient ($\Delta v/v = 0.004$) inherent in ZnO/Si devices that utilize the first Rayleigh mode and thin ZnO films (1.6 μm). However, larger coupling coefficients [16]

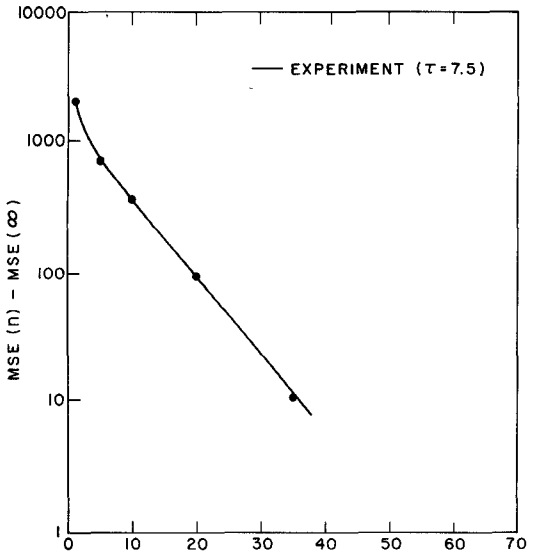

Fig. 10. Mean square error during adapting process.

($\Delta v/v = 0.028$) are obtained when the second Rayleigh mode (Sezawa mode) is used in devices which have thicker ZnO films (8 μm). We have demonstrated Sezawa wave convolvers which had four times the bandwidth (32 MHz) of the device described in this paper. We are presently developing broad-band Sezawa wave storage correlators with the intent of demonstrating improved SAW adaptive filters. The ultimate bandwidth to be expected from such devices should be at least 60 MHz. The diode array length (3 μs) is also a limitation since we cannot adapt signals which are longer than this. Also, since the correlation signal is truncated, the filter output is distorted. Since 3-in silicon wafer processing is a standard process, storage correlators with 10-μs signal processing capability should be easily attainable.

The two limitations indicated above are manifestations of the fact that if the correlator had a larger time–bandwidth product than 24, then it would equivalently have more taps and could adapt a broader class of signals. Time–bandwidth products of 1000 or more are possible with the use of present technology. Note, however, that (26) predicts that if the number of taps is increased, then the convergence time also increases (for a given level of misadjustment). Thus a larger number of taps is not desirable for applications in which the distortion is changing rapidly. For example, if the timing or amplitude of the echo significantly changes over a time period of 200 μs (10 iterations), then a larger number of taps would not be desirable.

The maximum output dynamic range of the device used here is 35 dB [12]. The dynamic range exhibited in this application is only 20 dB (Fig. 5), since this is an adapting process and the input power levels must be low enough that saturation of the output does not occur. The two major sources of spurious signals are: 1) capacitive coupling of the plate signal to the output acoustic port; and 2) spurious surface waves generated by the plate signal. Direct RF coupling can be reduced below the other signal levels with proper grounding and shielding techniques. Spurious SAW generation would appear to limit the maximum dynamic range of this device to 60 dB. Generation of bulk waves has not limited the dynamic range of monolithic Rayleigh wave correlators. However, they may be important in Sezawa wave correlators, since the ZnO film is thicker and the acoustic bandwidth is broader.

If a delay line with the same delay as the feedback delay line is used to delay the write signal, then the carrier frequency does not have to be adjusted to obtain convergence ($\Delta\omega \to \infty$ in (18)).

V. Conclusions

It was demonstrated that a -6-dB echo could be suppressed to -15 dB in 200 μs (10 iterations). The sidelobe level of the impulse response of a 1.25-MHz acoustic bulk transducer can be reduced from -2 to -10 dB with adaptive filtering.

The experimental results are on the whole in excellent agreement with the computer simulations. Thus it appears that the storage correlator is being operated in the optimum manner and that the only major distortion introduced by the storage correlator is the presence of the threshold and clipping levels.

There are many advantages of using a storage correlator to implement the clipped LMS algorithm for adaptive filtering. Only two connections are needed for a device which can correlate, convolve, store, and add broad-band RF signals in real time. The device is small (1 cm^2) and has the potential of much broader bandwidths (100 MHz) than is obtainable with digital techniques. The device is far faster in operation than any competitive inverse filter with its bandwidth.

Acknowledgment

The authors wish to thank C. Williams, B. T. Khuri-Yakub, and H. Tuan for valuable discussion and suggestions.

References

[1] J. M. McCool and B. Widrow, "Principles and applications of adaptive filters," in *IEEE Conf. Publ.*, vol. 144, pp. 84–95, 1976.
[2] D. Corl, "A C.T.D. adaptive inverse filter," *Electron. Lett.*, vol. 14, pp. 60–62, 1978.
[3] R. W. Lucky, "Automatic equalization for digital communications," *Bell Syst. Tech. J.*, vol. 66, pp. 547–588, 1965.
[4] P. M. Grant and G. S. Kino, "Adaptive filter based on SAW monolithic storage correlators," *Electron. Lett.*, vol. 14, pp. 562–564, 1978.
[5] D. Behar *et al.*, "The use of a programmable filter for inverse filtering," *Electron. Lett.*, vol. 16, no. 3, pp. 88–89, 1980.
[6] B. K. Ahuja *et al.*, "A sampled analog MOS LSI adaptive filter," *IEEE J. Solid-State Circuits*, vol. SC-14, pp 148–154, 1979.
[7] D. F. Barbe *et al.*, "Signal processing with charge coupled devices," *IEEE J. Solid-State Circuits*, vol. SC-13, pp. 34–51, 1978.
[8] W. K. Masenten, "Adaptive processing for spread spectrum communications systems," Hughes Aircraft Co., Rep. TP 77-14-22, Sept. 1977.
[9] D. Behar *et al.*, "The storage correlator as an adaptive inverse filter," *Electron. Lett.*, vol. 16, no. 4, pp. 130–131, 1980.

[10] K. A. Ingebritsen *et al.*, "A Schottky diode acoustic memory and correlator," *Appl. Phys. Lett.*, vol. 26, pp. 596–598, 1975.
[11] C. Maerfelt and Ph. Defranould, "A surface wave memory device using pn diodes," in *IEEE Ultrasonics Symp. Proc.*, pp. 209–211, 1975.
[12] H. C. Tuan *et al.*, "A new zinc oxide on silicon monolithic storage correlator," in *IEEE Ultrasonics Symp. Proc.*, pp. 496–499, 1977.
[13] H. C. Tuan, J. E. Bowers, and G. S. Kino, "Theoretical and experimental results for monolithic SAW memory correlators," *IEEE Trans. Sonics Ultrason.*, vol. SU-27, pp. 360–369, Nov. 1980.
[14] B. Widrow *et al.*, "Stationary and nonstationary learning characteristics of the LMS adaptive filter," *Proc. IEEE*, vol. 64, pp. 1151–1162, 1976.
[15] B. Widrow and J. M. McCool, "A comparison of adaptive algorithms based on the methods of steepest descent and random search," *IEEE Trans. Antennas Propagat.*, vol. AP-24, pp. 616–637, 1976.
[16] J. E. Bowers, B. T. Khuri-Yakub, and G. S. Kino, "Broadband efficient thin film Sezawa wave interdigital transducers," *Appl. Phys. Lett.*, vol. 36, pp. 806–807, 1980.

Surface-Acoustic-Wave Random-Access Memories

GIANFRANCO F. MANES

Abstract—**An acoustic tapped-delay line (TDL) undermultiplexer control exhibits random-access-memory (RAM) capability; programmable time compression/expansion is achieved by controlling the difference between tap switching interval and intertap delay. A serial-in/parallel-out configuration can perform spectral compression of high input bandwidths, while requiring a single sampling operation to be performed, at the output data rate; dual properties are demonstrated by a parallel-in/serial-out organized RAM used for time compression. A new powerful N-phase configuration is discussed, which allows the intrinsic switching capability of multiplexers employed to be increased by N, while offering high dynamic range capability.**

The basic operation of the new technique is discussed, some theoretical aspects are investigated, and various effective configurations are described. In particular, the natural format of the time contracted/segmented output from a nonlinear convolver, asynchronously operated, is recovered; a clock-programmable bandpass filter is demonstrated, based on complementary time compression expansion. Extension to read-only memory (ROM) is briefly outlighted, with reference to frequency synthesis.

Finally, processing of signals in baseband format is demonstrated using acoustic TDL's, via a simple modulation technique, which increases flexibility and the potential attraction of the new technique.

I. Introduction

SURFACE-ACOUSTIC-WAVE (SAW) tapped-delay lines (TDL) have represented the first attractive implementation of analog transversal structures, operating in the intermediate frequency range, providing almost ideal time-domain discrete access, and offering unique signal-processing capabilities in terms of maximum equivalent sampling rate and BT product. The advent of charge-transfer devices (CTD) has more recently permitted the realization of analog integrated transversal structures in the complementary baseband frequency range. CTD's, where data samples are stored in the form of charge packets and transferred in clocked shift-register fashion, exhibit random-access-memory (RAM) operation capability, thus forming an ideal candidate for applications requiring programmability at clock rates not exceeding a few megahertz. Conversely, surface-acoustic-wave (SAW) devices, where data are transfered in the form of a fixed-velocity piezoelectric wave and collected by a rigid tapping structure, appear inherently prevented from application to the important class of programmable signal-processing operations. A relative degree of programmability has been so far achieved only by special SAW devices, based on nonlinear interaction of acoustic waves in the piezoelectric substrate [1] or in coupled diode arrays [2] or in doped semiconductors [1].

The inherent limitations associated with the rigid time-access structure of SAW TDL's can be circumvented, however, by a recently demonstrated technique [3], [4] basically consisting in demultiplexing the parallel available data at a programmable rate through an analog multiplexer. The technique results in a SAW-based RAM, exhibiting clock-programmable time-compression/expansion and time-delay capability, relying on the particular sampling operation involved rather than on a new physical mechanism.

A number of unique configurations based on this tech-

Manuscript received May 1, 1980. This work was supported under contract with the special project on Biomedical Technologies of the National Research Council.

The author is with Istituto di Elettronica, Universitá di Firenze, Florence, Italy.

0018-9480/81/0500-0498$00.75 ©1981 IEEE